J Mater Sci: Mater Med (2008) 19:159–166
DOI 10.1007/s10856-006-0102-1

Extracorporeal hydroxyapatite-chamber for bone and biomaterial studies

Luigi Tarallo · Davide Zaffe · Roberto Adani · Adriano Krajewski · Antonio Ravaglioli

Received: 9 May 2006 / Accepted: 4 December 2006 / Published online: 28 June 2007
© Springer Science+Business Media, LLC 2007

Abstract Hydroxyapatite (HA) spherules and autologous bone (AB) with a central vascular pedicle were housed inside an HA-chamber to form the skeletal segment of specific shape. Experimental chambers were then inserted in a pocket between medial thigh muscles in 13 New Zealand male rabbits for 3 months. Three graft group were scheduled: (A) HA and AB without vascular pedicle, (B) HA with vascular pedicle, (C) HA and AB with vascular pedicle. At term, histology showed tissue and cellular degeneration in group A chambers. Due to spherules coalescence, fibrous tissue is formed in group B chambers. Group C chambers contained living osteocytes in the implanted bone, several newly formed vessels in soft tissue, bone and partial hydroxyapatite erosions. New bone was formed in apposition to both autologous bone and hydroxyapatite. Our study suggests that this experimental model could be used to grow adequately sized vascularized skeletal segments.

L. Tarallo · R. Adani
Department of Emergency/Urgency, Section of Orthopaedic Clinic, University of Modena and Reggio Emilia, Via del pozzo 71, Policlinico, Modena 41100, Italy

D. Zaffe (✉)
Department of Anatomy and Histology, Section of Human Anatomy, University of Modena and Reggio Emilia, Via del pozzo 71, Policlinico, Modena 41100, Italy
e-mail: zaffe@unimore.it

A. Krajewski · A. Ravaglioli
ISTEC, Via Granarolo 64, Faenza, RA 48018, Italy

Introduction

Autologous bone is currently regarded the gold standard for grafts by orthopedic and maxillo-facial surgeons [1, 2]. When the skeletal defect is small, autologous bone grafting is the best choice. Large defects need greater amount of autologous bone, which is collected as particulate and cannot always be harvested in adequate amounts. The use of a prefabricated skeletal segment made of biomaterial, with or without autologous bone, may help overcome these drawbacks.

The principle of tissue prefabrication has been consolidated over recent years [3–5]. Prefabrication aims to obtain a transferable material (skin, muscle, bony, composite), with features similar to the defect to be repaired, in order to reduce morbidity and improve the efficacy of reconstruction. In the revascularization of the carpal lunate bone in Kienböck's disease [6–8], bone neovascularization by implant of vascular pedicle is today a well-known and common clinical practice. This therapeutic option follows works by several authors [9–11] on bony neovascularization by vascular implantation in experiment animal models. In a previous study [12], we report the proliferation of a specimen of rabbit iliac crest with vascular bundle, when placed subcutaneoulsly; small amounts of new bone were formed on the surfaces of the extracorporeal skeletal segments, 8 weeks after vessels insertion.

Extracorporeal vascularized chambers have been studied since 1985 using metallic or plastic containers [13, 14]. Ceramic chamber were then used in rabbits to obtain vascularized bone grafts with demineralized bone [15] or porous calcium pyrophosphate [16]. The latter type of chamber produced better results, probably because more skeletally biocompatible.

The purpose of this study was to assess the feasibility of a vascularized bone graft, of specific size and shape, using an extracorporeal ceramic chamber made of dense hydroxyapatite (HA) in the rabbit. The HA-chamber contained an axially blood vessel and was filled with a mixture of autologous bone and spherules of dense hydroxyapatite, particularly suitable as bone substitute [17–20]. Histology was assessed 12 weeks after surgery, with steady-state bone processes. This work was also a pilot study on the use of an experimental animal such as rabbit, which has enhanced bone metabolism and reactivity [19] and implant conditions approaching those found in humans, for biomaterial bench-testing.

Materials and methods

Thirteen male New Zealand white rabbits (one-year-old, weighting 4.5–5.5 kg, S. Morini, S. Polo d'Enza RE, Italy) were used to analyze the behavior of implanted HA-chambers; the Italian rules on breeding, housing and animal treatment were adhered to.

Chambers (15 mm outer diameter, 12 mm inner diameter and 15 mm length) were made by gluing together three hydroxyapatite parts: a hollow cylinder and two disks (Fig. 1A). The full density hydroxyapatite chambers were accomplished by extrusion molding technology using dense water-based slurries. Table 1 reports the composition of the slurry mixture. Hydroxyapatite [$Ca_5(PO_4)_3OH$; acronym HA] biograde powder was first annealed at 900 °C for 1 h in a laboratory kiln to lower the specific surface and enhance the rheological properties of the paste. The organic components of Table 1 were added to the previously annealed HA powder and the mixture obtained was stirred for 2 h in a cooled jar with shovel blender. The obtained dense and pliable paste was then placed in a piston-extruder machine [proprietary design, manufactured under contract by Bettini S.p.A. of Montemarenzio (Italy)] to form cylindrical molds shaped by extrusion technology. The ingredients were amalgamated in a stainless steel blade mixer [proprietary design by ISTEC-CNR] until homogeneous (about 1 h) and soaked 2–4 h to allow rearrangement of water and polymeric molecules of HA particles in the plastic mass. Extrusion was carried out by suitable equipment under controlled conditions (piston diameter = 40 mm; pressure = 2 MPa; extrusion piston speed = 2 mm/s) and a draw-plate of the appropriate size. The cylindrical-shaped green bodies were then dried in a moisture-controlled environment for several days. The disks (15 mm diameter and 500 μm thickness) were manufactured, using the same HA annealing powders used for extrusion, die pressed into thin disks by stainless steel equipment [proprietary design by ISTEC-CNR] at a pressure of 4 MPa. All the ceramics were subsequently sintered at 1250 °C for 1 h (ramp: 50 °C/h). Contraction of the ceramic component during the sintering process, from the green bodies to the sintered cylinders, was evaluated (~22% linear) and taken into account to reach the target diameter of the cylinder and disks. A thin bronze plate made the cold-drawn mouth of the extruder with circular cleft diameter augmented by the percent contraction over the final target diameter of the chambers. The hollow cylinders and perforated disks (15 mm outer diameter, 8 mm inner diameter, 500 μm thickness) were cut from the corresponding hydroxyapatite cylinders (Fig. 1). All finishing processes, such as polishing, shaping and sizing were performed on the parts after sintering, utilizing diamonded pastes and papers and proprietary polishing devices. The perforated disk was preoperatively attached to the cylindrical wall using cyanoacrylate glue.

Rabbits were divided into three groups depending on the packing of the ceramic chambers (autologous—iliac crest—cancellous bone and/or HA-spherules, 600–900 micron diameter, FIN-CERAMICA FAENZA, Faenza RA, Italy) and to the presence of the vascular pedicle. *Group A* consisted of 3 rabbits (HA & bone, without vascular pedicle), *group B* of 5 rabbits (HA-spherules surrounding the vascular pedicle), and *group C* of 5 rabbits (HA & autologous bone surrounding the vascular pedicle). Experiments were run at the Breeding Department, Medical

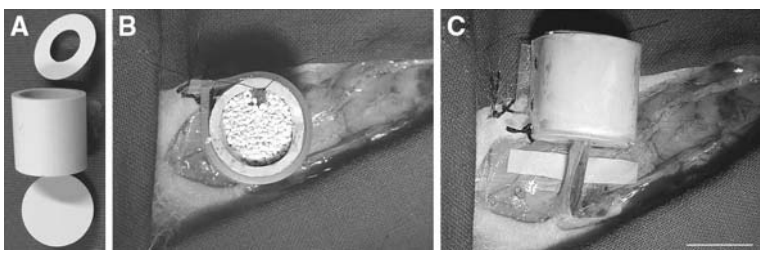

Fig. 1 Each chamber consists of three hydroxyapatite parts, a cylinder and two disks (**A**). Note in **B** the chamber, wrapped in a silicone envelope, which contains the vascular pedicle supported by a nylon suture and surrounded by hydroxyapatite spherules. In **C**, the chamber is fastened to the muscle fascia

Table 1 Composition of starting mixture

Component (Manufacturer)	Treatment	Scope	Quantity (wt %)
Hydroxyapatite (Riedel de Haën—Seelze, Germany)	Annealed for 1 h at 900 °C	–	46.51
Benzyl alcohol (Carlo Erba Reagenti—Rodano MI, Italy)	–	Lubricant	0.93
Glycerol (Merck KGaA—Darmstadt, Germany)	–	Lubricant	0.45
Methyl-HydroxyMethyl-Cellulose (Aqualon group—Alizay, France)	–	Agglutinant/binding	0.45
Zusoplast (Zschimmer & Schwarz—Lahnstein/Rhein, Germany)	–	Plastifier/emulsifier	0.45
PolyEthylenGlycol 400 (Carlo Erba Reagenti—Rodano MI, Italy)	–	Densifier	0.06
Bidistilled water	–	Eluant	37.2

Center of Modena, under general ketamine/xylazine anesthesia, and sterile conditions. The right saphenous vascular pedicle, consisting of a superficial artery and adjacent vein were exposed for about 7 cm from the upper third of the thigh, as reported elsewhere [12]. The vascular pedicle with the distal part fastened by Nylon 6/0 suture was inserted axially into the hydroxyapatite chamber (wrapped in 1 mm-thick silicone foil to isolate the system) through the hole in the disk (Fig. 1B). Various grafts were used to fill the chamber space. An accurate mixture of 50% HA and 50% autologous bone was prepared for the combined graft. Bone (about 2 cm^3 per rabbit), previously harvested from the iliac crest [12] without power instrument to avoid heat damage, was fragmented to achieve a homogeneous mixture with HA spherules. The HA-plug, lined with silicone foil, was intraoperatively glued to the hydroxyapatite chamber. The whole system (V = 2.7 cm^3; Wt = 5–6 g, when filled with only HA) was then fastened in a subcutaneous pocket on the medial surface of the right thigh (Fig. 1C). A wide-spectrum antibiotic was administered for 3 days after surgery. Rabbits were euthanized (N-[2-m-methoxyphenyl)-2-ethyl-buthyl-(1)]-γ-hydroxybutyric amide + 4,4′-methylen-bis(cycloexyl-trimethylammonium iodate) 3 months after the surgery. A patency test of the implanted vascular axis was performed intraoperatively in all animals before harvesting the hydroxyapatite chambers.

The HA-chambers were fixed in 4% buffered (pH 7.2) paraformaldehyde (all reagents Fluka Chemie AG, Buchs, Switzerland) for 4 h, and PMMA embedded without decalcifications as previously described [21]. Longitudinal thick sections (200 μm thick) of the chambers were obtained using a diamond-saw microtome (1600 Leica, Wetzlar, Germany), whereas thin sections (5 μm thickness) were cut using a tungsten carbide-blade microtome (Autocut1150, Reichert-Jung GmbH, Nußloc, Germany). Thick sections were reduced in thickness (80–100 μm) by grinding, and then surface polished. These sections were microradiographed (MR3000, Italstructures, Riva del Garda TN, Italy) on Ilford EM film (high contrast microradiographs) or Kodak SO343 film (high resolution microradiographs) and analyzed under optical and scanning electron microscope, after gold sputtering of the section surface as described elsewhere [22]. Thin sections were stained with Toluidine Blue, Gomori trichrome or Solochrome cyanine/Congo red methods. The Trabecular Bone Volume (TBV) index of the amount of bone tissue [23], newly formed on HA spherules, was calculated on microradiographs using an image analyzer (VIDAS, Carl Zeiss Jena GmbH, Jena, Germany).

Results

Clinical inspection 3 months after surgery revealed a recurrent displacement of the chamber from its starting location. Chambers were found in subcutaneous tissue rather than adhering to the fascial tissue of the muscle pocket. A thin layer of fibrous tissue connected to perivascular connective tissue covered the silicone envelope of the harvested chambers.

Group A (HA & bone, without vascular pedicle)

Autologous bone fragments and hydroxyapatite (HA) spherules (Fig. 2A) were scattered throughout the chambers. HA and bone trabeculae were in the same position where they had been placed 3 months before and remained the same size and shape (Fig. 2A). Chambers displayed degenerative processes: no living tissue surrounded HA spherules or bone. Bone marrow between the bone trabeculae degenerated completely (Fig. 3A). Only empty osteocyte-lacunae were observed in the bone trabeculae of chambers of this group (Fig. 3A). The TBV (HA & bone), evaluated on microradiographs of the central portion of each chamber, was about 43% (HA = 25.5 ± 3.1–Bone = 17.7 ± 2.6—-m ± S.E.) in chambers of this group (Fig. 9).

Group B (HA-spherules surrounding the vascular pedicle)

Spherules clumped together to form a nearly compact mass inside the chamber (Fig. 2B). Spacing among spherules

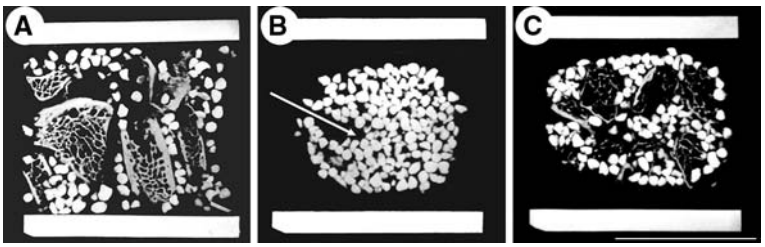

Fig. 2 Microradiograph of thick sections of chambers in: **A** = group A (no vessel); **B** = group B (vessel +HA); **C** = group C (Vessel + HA & bone). The arrow in **B** indicates the location of the vascular pedicle. Note the thinning of bone trabeculae in **C**. Bar = 10 mm

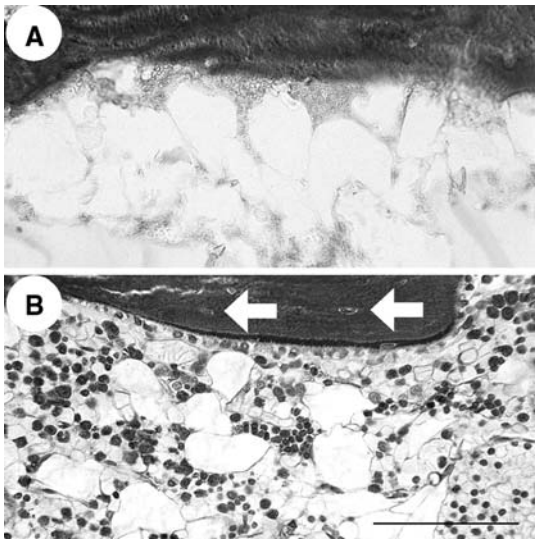

Fig. 3 Thin sections of chambers in group A (**A**) and C (**B**) displaying autologous bone and medullary tissue. The arrows in B point to two living osteocytes of the implanted bone. Note the different appearance of the medullary tissue. Gomori trichrome stain. Bar = 100 μm

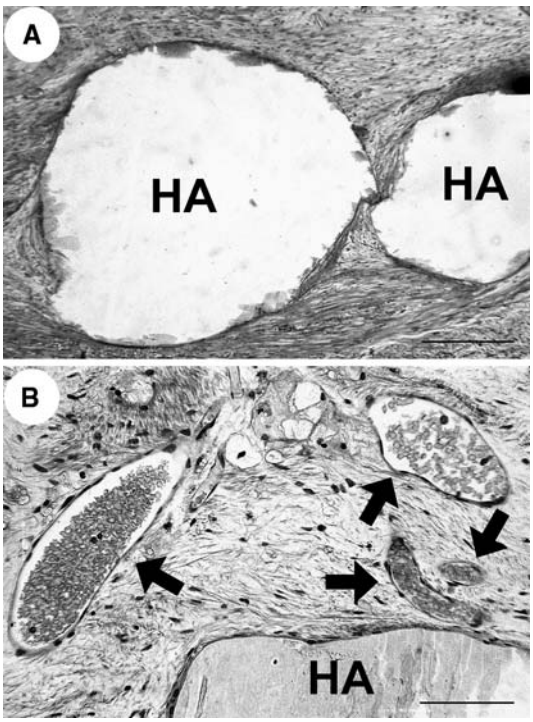

Fig. 4 Thin sections of chambers in group B (**A**) and C (**B**) displaying hydroxyapatite spherules surrounded by fibrous tissue. The arrows in **B** point to several vessels of the soft tissue surrounding spherules in group **C**. Gomori trichrome stain. Bars A = 250 μm, B = 100 μm

was greatly reduced. A slightly greater amount of fibrous tissue was observed near the vascular pedicle (arrow in Fig. 2B). Hydroxyapatite spherules were surrounded by dense fibrous tissue that completely filled the spaces amid the spherules. Consequently, this layer was normally thin and became thicker closer to the vascular pedicle. Only few and small vessels were observed around the HA spherules in this fibrous tissue (Fig. 4A). The TBV of the central portion of each chamber (Fig. 9), corresponding to the only HA in chambers of this group, was slightly greater than 40% (40.4 ± 2,1—m ± S.E.).

Group C (HA & bone surrounding the vascular pedicle)

Spherule clumping in the chambers was similar to that observed in group B, but more soft tissue was observed amid the spherules (Fig. 2C). Autologous bone trabeculae were markedly thinned even though their content was probably similar to that at the starting (Fig. 2C). Contrary to group A, osteocyte-lacunae were filled by living cells in all bone of chambers of this group, and all cells and intercellular materials of medullary tissues were preserved (Fig. 3B). Contrary to group B, large vessels were found both inside the medullary tissue surrounding bone trabeculae and in fibrous sheath of different thickness surrounding HA spherules (Fig. 4B).

An appreciable portion of autologous bone inserted in chambers of this group showed the result of osteoclast activity: bone trabeculae had a pitted surface and erosion channels inside the bone (Fig. 5A). Several Howship lacunae, produced by multinuclear cells (osteoclasts), characterized the autologous bone surface. Osteoclasts were found not only resorbing the inserted autologous

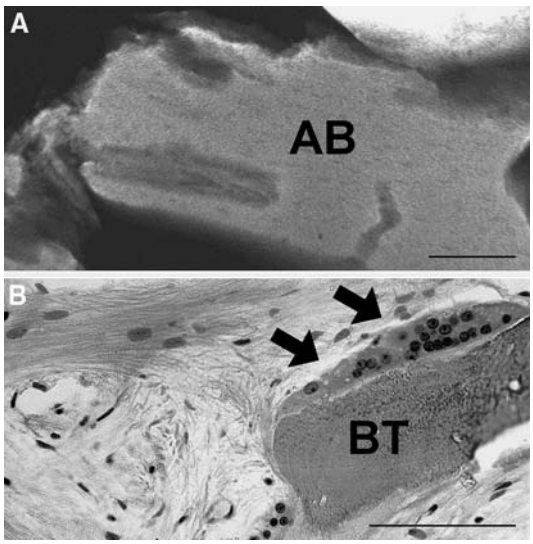

Fig. 5 Microradiograph (**A**) and thin section (**B**) display a segment of implanted autologous bone (AB) from group **C** chambers. Note the pitted profile and the channel of bone in **A**. The arrows in **B** point to an osteoclast group eroding the tip of a newly formed bone trabecula (BT). Solochrome cyanine/Congo red stain. Bars: A = B = 100 μm

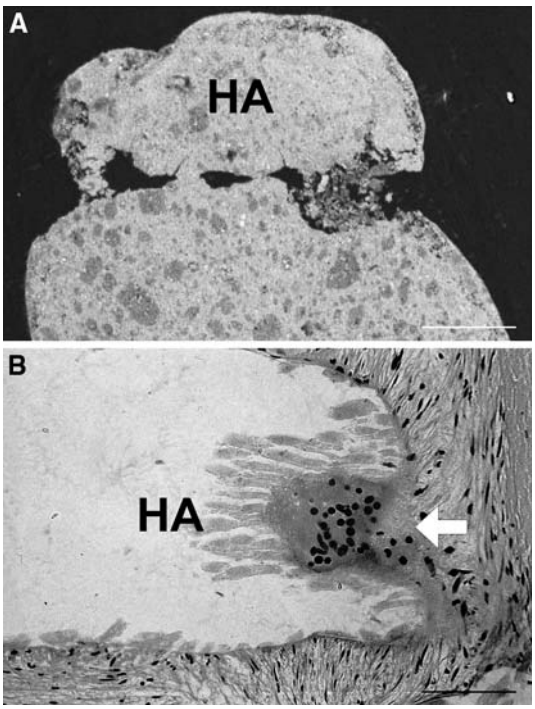

Fig. 6 SEM micrograph (**A**) and thin section (**B**) display hydroxyapatite spherules in group **C** chambers. Note the darker appearance, i.e. demineralization, of the fragmented material inside the HA pocket in **A**. The arrow in B points to an osteoclast group eroding HA, forming a pocket. Solochrome cyanine/Congo red stain. Bars: A = B = 100 μm

bone, but also on newly formed bone (Fig. 5B). Evidence of osteoclast-like cell-activities was observed in some hydroxyapatite spherules (Fig. 6A). These multinuclear cells were able to resorb hydroxyapatite (Fig. 6B), leading to demineralization, and form channels in the spherules. Some spherules lost their smooth contours and showed pitting on their surface, evidence of macrophagic activity.

Osteoblasts formed new bone in apposition to the surface of both autologous bone, which always housed living osteocytes (Fig. 7A), and hydroxyapatite spherules (Fig. 8A). Dynamic osteogenesis [24] on preexisting skeletal support (bone or HA) was sometimes observed, even if static osteogenesis [24] was the common process. Osteogenetic processes involved 20–25% of autologous bone persisting after osteoclast activity. New bone with woven fibered structure was formed in apposition to both resorbed and unresorbed bone surfaces. Sometimes, bone with a more regular structure, such as lamellar bone, was formed in apposition to the surface of pre-existing and partially resorbed lamellar bone (Fig. 7B, C). Newly formed bone sometimes bridged autologous bone to HA spherules (Fig. 7A). This bone nearly always had a woven structure with high cellularity. Osteoblasts sometimes directly formed new bone in apposition to the HA surface (Fig. 8A, B). New bone had a woven structure and contained typical irregularly shaped osteocytes. Ellipsoidal osteocytes, characteristic of more ordered bone (parallel fibered or lamellar), were sometimes observed in bone formed in apposition to HA spherules. New bone frequently connected autologous bone trabeculae with HA spherules and spherules, fixing them into small trabeculae–spherules meshwork (Fig. 8C).

The HA (22.5 ± 1.2—m ± S.E.) had a TBV value similar to that of group A chambers, whereas bone (9.9 ± 0.9—m ± S.E.) displayed a reduced TBV value. Nevertheless, a small amount of new bone formation (3.1 ± 0.2—m ± S.E.) was recorded (Fig. 9).

Discussion and conclusions

The possibility to grow preformed skeletal segments using either bone or biomaterials seems corroborated by the results of this rabbit model. Dislocation of the experimental chambers in all rabbits is probably caused by the relatively high mass of the system, in particular when filled only with hydroxyapatite. Nevertheless, the observed displacement does not seem to influence the angiogenic, osteogenetic and osteolytic processes.

Several events occur inside the chambers:

(a) cell and tissue vitality are maintained only when the vascular pedicle is patent;
(b) all inserted autologous bone undergoes osteoclastic erosion to some extent;

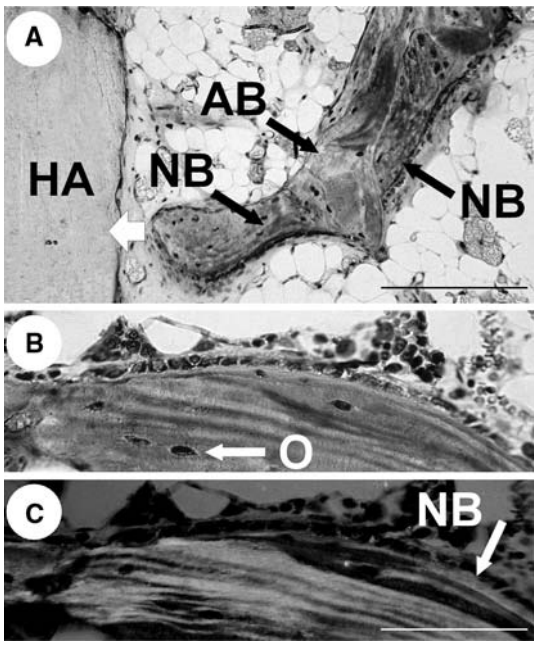

Fig. 7 Thin sections displaying the new bone (NB) formed in apposition to autologous bone (AB) in group **C** chambers. The new bone of A, mostly woven structured, grows toward the spherule (arrow) to connect hydroxyapatite (HA). **B** (ordinary light) and **C** (polarized light) show lamellar autologous bone, containing living osteocytes (O), whereas osteoblasts form new lamellar bone (NB). Toluidine blue stain. Bars: A = 250 μm, B = C = 100 μ

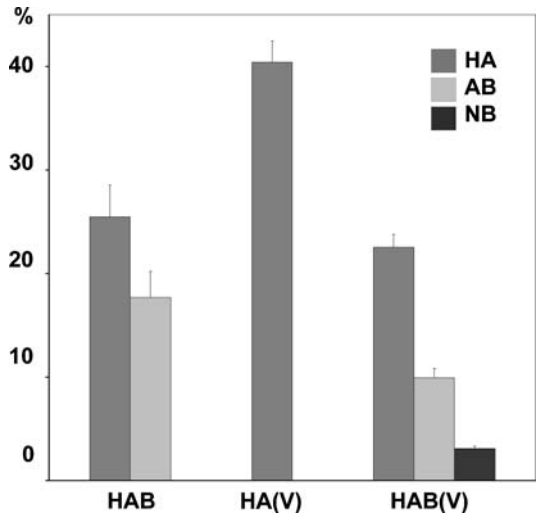

Fig. 9 Graph (mean + standardd error) illustrating the TBV behavior (express as %) of the mineralized component in **A**, **B** and **C** group chambers. (HA = hydroxyapatite spherules; AB = autologous bone; NB = newly formed bone)

(c) a part of hydroxyapatite spherules undergoes resorption by multinuclear cells;
(d) autologous bone, persisting after osteoclast activity, acts as scaffold to a small but significant formation of new bone;
(e) most hydroxyapatite spherules undergo osteogenic processes that transform the distinct spherules into complex bone—hydroxyapatite meshwork.

The absence of living material in chambers without the vascular pedicle confirms the capability of the silicone envelope to completely isolate the system. We previously described this effect in a study on revascularization of a bone segment [12], but in that situation isolation of the system was easier. Due to the chamber conformation, we could not be sure of complete system isolation, as stated by the results. Therefore all cellular activities recorded (angiogenesis, osteoclasia, osteogenesis) were due to cells supplied by the vascular pedicle. Biological fluids and cells cross the perivascular tissue and reach bone or hydroxyapatite. The former guarantee the vitality of the living tissues inserted (bone and soft tissues), the latter act on the above-mentioned processes.

Though it may seem remarkable, bone erosion due to osteoclastic activity is a normal behavior that is particularly enhanced in an unloaded system. Bone erosion is normal in autologous bone grafting in humans. In our experimental system, bone osteoclasia is particularly enhanced because pre-osteoclastic cells are recruited before pre-osteoblasts.

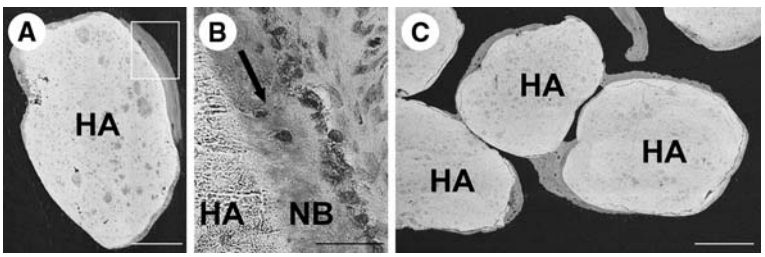

Fig. 8 SEM micrographs (**A** and **C**) and thin section (**B**) display the bone formed in apposition to hydroxyapatite spherules in group **C** chambers. The boxed inset in **A** corresponds to a detail at higher magnification of image **B**. Note in B how osteoblasts form new woven bone (NB), containing the typical irregularly-shaped osteocytes (arrow), in direct apposition to the hydroxyapatite (HA) surface. Newly formed bone (**C**) joins the HA spherules forming a calcified meshwork. Toluidine blue stain. Bars: A = 100 μm; B = 50 μm; C = 250 μm

This clastic predilection is probably favored by the extramusculoskeletal site of implant switched to osteoblastic activity only after a large amount of calcium ions have been released. The particular design of our experimental model may intensify the initial delay of osteogenetic processes in rabbit. This is not necessarily a negative effect, because experimental animals (mouse, rat and rabbit) have a faster reaction time than humans [18]. Our model suggests a way to restore osteoblastic reactivity to that reported in humans.

Resorption of hydroxyapatite spherules, though enhanced over that of implants of good-quality hydroxyapatite, is a normal event that also occurs in the long term in hydroxyapatite implants. Strong hydroxyapatite aggression in our system is probably due to intense osteoclastic or preosteoclastic recruitment. We can postulate that calcium release by defective hydroxyapatite spherules may favor clastic attraction instead of osteoblastic stimulation; however, here the hypothesis of poor chemical composition of hydroxyapatite as a cause of osteoclastic-like cells activity can be ruled out by the tests on hydroxyapatite quality prior to implant. Moreover, most of the hydroxyapatite spherules are basically unaltered. TRAP-positive osteoclastic-like cells erode and almost completely destroy all hydroxyapatite formations having a wrong chemical composition [25]. We can also postulate that calcium release due to these clastic activities on small defective parts of hydroxyapatite spherules may have a positive effect on osteoblast stimulation and bone formation on hydroxyapatite surface.

Though results showed good osteostimulative capabilities of the tested HA, they also highlight a negative effect probably due to HA density. The formation of a nearly compact mass inside group B chambers and the small new bone formation in group C chambers can probably be ascribed to the relatively high mass of HA granules. Rabbit movements, for instance hopping, probably led to spherule displacements thus perturbing all biological processes, including osteogenesis. The use of a porous hydroxyapatite [20] (which reduces the relative mass of the graft and increases osteoconductive surfaces) and sealing of granules [26] might improve the results.

In conclusion, our experimental system is functional for both biomaterial evaluation and tissue engineering. The use of vascularized chamber with characteristics similar to those of bone mineral lead to a weak biological response in this experimental animal, which has a very high bone metabolism and capability for biomaterial engulfing [27]. Our study describes an experimental model that combines the prefabricated neovascularized bone with biomaterials to obtain a bone graft of predefined size and shape. We believe that this experimental surgical method may be applicable in clinical conditions characterized by the need to reconstruct peculiar bony defects, such as in the upper limb surgery. Further prospects for the present study could be an integration of surgical technique and biomedical engineering with the use of cell culture lines such as osteoblasts, chondrocytes and strong stem cells combined with support frames made of biodegradable and biocompatible synthetic polymers.

Acknowledgements The authors wish to thank Mr. Vincenzo Molino for his remarkable technical assistance in animal care and treatment, and the "Centro interdipartimentale Grandi Strumenti" (CIGS) of the University of Modena e Reggio Emilia for SEM availability and assistance. The Research University Fund (FAR) of the Department of Anatomy and Histology, University of Modena and Reggio Emilia supported this investigation.

References

1. S. C. GAMRADT and J. R. LIEBERMAN, *Clin. Orthop. Relat. Res.* **417** (2003) 183
2. J. N. GRAUER, J. M. BEINER, B. K. KWON and A. R. VACCARO, *BioDrugs* **17** (2003) 391
3. J UPTON, N. FERRARO, G. HEALY, R. KHOURI and C. MERREL, *Plast. Reconstr. Surg.* **94** (1994) 573
4. Y. CAO, J. P. VACANTI, K. T. PAIGE, J. UPON and C. A. VACANTI, *Plast. Reconstr. Surg.* **100** (1997) 297
5. N. ISOGAI, W. LANDIS, T. KIM, L. GERSTENFELD and J. UPTON, *J. Bone Joint Surg.* **81A** (1999) 306
6. Y. HORY, S. TAMAI, H. OKUDA, H. SAKAMOTO, T. TAKITA and K. MASUHARA, *J. Hand Surg.* **4** (1979) 23
7. J. H. GUO, *Ann. Plast. Surg.* **36** (1996) 133
8. G. M. GARTSMAN, A. J. WEILAND, J. R. MOORE and M. A. RANDOLPH, *J. Reconstr. Microsurg.* **1** (1985) 215
9. D. R. GILL, D. C. IRELAND, J. V. HURLEY and W. A. MORRISON, *J. Hand Surg*. **23A** (1998) 312
10. T. KASASHIMA, A. MINAMI, H. KATO and K. KANEDA, *J. Reconstr. Microsurg.* **16** (2000) 121
11. M. CELIK, S. TUNCER, U. EMEKLI and S. N. KESIM, *J. Oral Maxillofac. Surg.* **58** (2000) 292
12. R. BUSA, R. ADANI, C. CASTAGNETTI, D. ZAFFE and A. MINGIONE, *Microsurgery* **19** (1999) 289
13. H. NETTELBLAD, M. A. RANDOLPH, L. T. OSTRUP and T. I. WEILAND, *Plast. Reconstr. Surg.* **76** (1985) 851
14. S. MIZUMOTO, Y. INADA and A. J. WEILAND, *J. Reconstr. Microsurg.* **8** (1992) 325
15. S. MIZUMOTO, Y. INADA and A. J. WEILAND, *J. Reconstr. Microsurg.* **9** (1993) 441
16. C. C. LIN, C. J. LIAO, J. S. SUN, H. C. LIU and F. H. LIN, *Biomaterials* **17** (1996) 1133
17. A. MORONI, S. GIANNINI, D. ZAFFE, A. RAVAGLIOLI, A. KRAJEWSKI, A. VENTURINI, M. POMPILI, S. CANTAGALLI, V. PEZZUTO and L. TRINCHESE, *Bioceramics* Vol. 2. (Köln:Deutsche Keramische Gesellschaft e.V.; 1990), p. 125
18. D. ZAFFE, *BIOSIS Int. Soc. for Bio-Analog Skel Impl.* (Elztal-Dallau - D:Laub GmbH & Co.; 1992), p. 63
19. D. ZAFFE, S. GIANNINI, A. MORONI, A. KRAJEWSKI and A. RAVAGLIOLI, *Bioceramics and the Human Body* (London: Elsevier Sci Publ Ltd, 1992), p. 388
20. H. M. T. U. HERATH, L. DI SILVIO and J. R. G. EVANS *J. Appl. Biomater. Biomech.* **3** (2005) 192
21. D. ZAFFE, G. C. LEGHISSA, J. PRADELLI and A. R. BOTTICELLI, *J. Mater. Sci. Mater. Med.* **16** (2005) 789

22. C. BERTOLDI, J. PRADELLI, U. CONSOLO and D. ZAFFE, *J. Mater. Sci. Mater. Med.* **16** (2005) 857
23. A. M. PARFITT, M. K. DREZNER, F. H. GLORIEUX, J. A. KANIS, H. MALLUCHE and P. J. MEUNIER, *J. Bone Miner. Res.* **2** (1987) 595
24. M. FERRETTI, C. PALUMBO and G. MAROTTI, *Anat. Embryol.* **206** (2002) 21
25. D. ZAFFE, C. BERTOLDI and U. CONSOLO, *Biomaterials* **25** (2004) 3837
26. R. R. KANIA, A. MEUNIER, M. HAMADOUCHE, L. SEDEL and H. PETITE, *J. Biomed. Mater. Res.* **43** (1998) 38
27. A. CIGADA, G. De SANCTIS, A. M. GATTI, A. ROOS and D. ZAFFE, *J. Appl. Biomater.* **4** (1993) 39